JOURNAL OF MATERIALS SCIENCE **37** (2002) 1561 – 1573

Talc as nucleating agent of polypropylene: morphology induced by lamellar particles addition and interface mineral-matrix modelization

E. FERRAGE*, F. MARTIN
Equipe Géomarg, UMR 5563 du CNRS, LMTG, 39 Allées Jules Guesde, Université Paul Sabatier, 31000 Toulouse, France
E-mail: eric.ferrage@ujf-grenoble.fr

A. BOUDET
Centre d'Elaboration des Matériaux et d'Etudes Structurales CEMES, CNRS, 29 rue Jeanne Marvig 31055 Toulouse Cedex 4, France

S. PETIT
UMR 6532 du CNRS, Laboratoire 'Hydr'A.S.A.' Université de Poitiers, 40 Avenue du recteur Pineau, 86022 Poitiers Cedex, France

G. FOURTY, F. JOUFFRET
Talc de Luzenac S. A., BP 1162, F-31036 Toulouse Cedex, France

P. MICOUD, P. DE PARSEVAL, S. SALVI
Equipe Géomarg, UMR 5563 du CNRS, LMTG, 39 Allées Jules Guesde, Université Paul Sabatier, 31000 Toulouse, France

C. BOURGERETTE
Centre d'Elaboration des Matériaux et d'Etudes Structurales CEMES, CNRS, 29 rue Jeanne Marvig 31055 Toulouse Cedex 4, France

J. FERRET, Y. SAINT-GERARD, S. BURATTO
Talc de Luzenac S. A., BP 1162, F-31036 Toulouse Cedex, France

J. P. FORTUNE
Equipe Géomarg, UMR 5563 du CNRS, LMTG, 39 Allées Jules Guesde, Université Paul Sabatier, 31000 Toulouse, France

The efficiency of talc used as nucleating agent (0.5% by weight) in polypropylene (PP) was determined taking into account the particle size d_{50}, particle morphology and BET specific surface areas. These findings were compared to a mineral with similar properties, pyrophyllite. Talc samples with the finest particle sizes induce a significant increase in the starting crystallization temperature of PP and irrespective of the particle size d_{50}, pyrophyllite was found to be less efficient than talc. X-Ray results show that PP oriented crystallization due to talc or pyrophyllite addition, corresponds to an epitaxial growth whereby the mineral c^*-axis is merged with the PP b^*-axis. Microscopic observations revealed that in the presence of talc, nuclei density of PP increased strongly. In addition, a large number of nuclei was observed to appear everywhere on the talc surface. A PP-talc interface model is proposed by matching the (001) talc plane and the (010) PP plane. In this model, 3% of PP cell accommodation on talc is necessary with a 15° angle between PP chains elongation and the crystallographic directions of talc. Hexagonal rings on talc surface are believed to represent hydrogen bonds with PP methyl groupings. This fine structure relation between talc and PP is discussed, and is used to characterize the differences observed between the efficiency of talc and that of pyrophyllite.

**Present Address*: LGIT, Maison des Géosciences, BP 53, 38041 Grenoble Cedex 9, France.

1. Introduction

Nowadays, talc ores are very useful in a large number of industrial applications such as paper, paint, ceramics and polymers. In polymer applications talc is used as a filler in various amounts (20 to 40% by weight) in isotactic polypropylene homopolymer or copolymer. When talc is used under 3% by weight, it is no longer considered as a filler but as a nucleating agent. Usage of talc brings about several modifications of polypropylene (PP) properties, which increase the industrial interest for this particular composite. Talc contrarily to other minerals (e.g., calcite, serpentines, micas), has proved to be particularly efficient filler on the mechanical properties and macromolecular orientation of a composite [1–4]. Addition of talc to PP increases the starting crystallization temperature, inducing a very short processing time in injection moulding [5]. This processing time is reduced proportionally to the increase of talc concentration [6]. Studies have shown that the increase of PP nuclei number observed with talc was due to the nucleating ability of the substrate [7, 8], where the substrate could present active sites on the surface [9]. Using talc as filler involves modifications in crystallization of the resulting composite, inducing an increase of its mechanical properties [10, 11]. This modifications was attributed to a preferential orientation of talc particle and PP in composite [12–14]. PP can crystallize in 4 polymorphic components: in the α, β forms and more rarely in the γ and δ forms [15]. Fillers such as talc usually induce the α form in PP, however many organic agents also can promote the formation of α and β form [5, 16, 17].

For this study, we used several types of talc as nucleating agents (0.5% by weight) in polypropylene. A Differential Scanning Calorimeter (DSC) technique was used to measure starting crystallization temperatures of composites, talc producing the best increase of this temperature is preferred for saving time when industrial pieces are molded. Our results show that this thermal property is strongly influenced by the physical characteristics of talc samples (particle size d_{50}, BET specific surface area). X-ray diffraction (XRD) analyses were also used to characterize the PP macromolecular orientation of PP pressed films, knowing that the mechanical properties of composites are increased when PP in the composite is oriented.

To specify the efficiency of talc as nucleating agent in PP, we compared talc to pyrophyllite (aluminous phyllosilicate) and two organic agents (α and β) which are known to induce good properties to PP composite, although in some industrial applications talc is preferred for its lower cost. PP crystallization observations with and without talc were carried out to characterize macromolecular modifications and to localize PP nucleation on particle surface. Finally, we focused our attention on talc-PP interface to understand the efficiency of this mineral on PP nucleation.

2. Experimental procedure

2.1. Starting materials

Polypropylene used in this study was homoisotactic polypropylene PPR 0160, produced by Targor Co., containing 0.25% stabilizing Irganox B225. In our experiments, stabilized PP was mixed with 0.5% nucleating agent sample (see below).

2.2. Nucleating agent sample description

2.2.1. Talc and pyrophyllite structure

Talc and pyrophyllite are 2 : 1 layer clays of the same phyllosilicate family which link two tetrahedral sheets with one octahedral sheet in their structure. Talc represents the trioctahedral magnesium end member with the formula: $Mg_3Si_4O_{10}(OH)_2$, while pyrophyllite is the dioctahedral aluminous end member with the formula: $Al_2Si_4O_{10}(OH)_2$.

Pioneering studies described talc as a monoclinic cell, with C-1 space group [18]. More recently, talc structure was described as triclinic [19], and subsequently pseudomonoclinic Cc with a P-1 space group [20]. Some structural distortions appear in layer silicates due to a structural accommodation between the tetrahedral sheet and the octahedral sheet as tetrahedral rotations and tilt of tetrahedra in the basal oxygen surface [21]. In talc, the tetrahedral rotation is 3.6° and the basal oxygen surface is nearly planar.

The single crystal structure of pyrophyllite has been described as similar to that of talc [22]. Due to the crystallochemistry difference, notably one octahedra vacancy, distortions in the (a, b) plane and along the c^* axis are more important in pyrophyllite than in talc. These include a tetrahedral rotation angle around 10.2° [23], with tetrahedra being tilted by about 4° and causing a strong corrugation to the basal surface of this mineral.

2.2.2. Lamellar nucleating agents

Several talc samples and two pyrophyllites specimens (see below) were used as nucleating agents of PP. Talcs of Spain, China and Italia are three commercial products from the "S.A. Talc de Luzenac" society (Toulouse, France), coming from the Léon, Haicheng and Val Chisone regions, respectively. Talc from Gabon was formed naturally by transformation of sepiolite. This sample, characterized by a particular structure, was provided from the collection of the research laboratory of "Luzenac Europe" (Toulouse, France). A last talc specimen was selected to observe the location of PP nucleation sites on talc surface. This sample is from Brazil and is characterized by long extended sheets on the (a, b) plane.

Two pyrophyllites were used: Pyro coll. from the collection of mineralogy (Toulouse, France) and Pyro luz from the laboratory research of "Luzenac Europe".

All samples were chosen for their physical characteristics (particle size d_{50}, B.E.T. specific surface area). They are also distinct by their different crystallinity: microcrystallinity corresponding to an heterogeneous arrangement of small flakes and macrocrystallinity with large flakes.

2.2.3. Organic nucleating agents

Two types of organic nucleating agents were used: ADK STAB NA-11 (Sodium 2,2′-methylene-bis-(4,6-di-tert-butylphenyl phosphate)) here in termed α nucleating agent, which induces crystallization of PP

in his α-form, and the NJ STAR NU-100 (N',N'-dicyclohexyl-2, 6-naphtalene dicarboxamide) here in β nucleating agent, which induces the β-form in PP. The two compounds are commercial products from "Palmarole" (France). PP, stabilizing and nucleating agents were mixed manually and introduced in a Clextral BC21 internal mixer to obtain compounds with desired concentrations.

2.3. Analytical techniques

Chemical compositions of talcs and Pyro luz powders were determined by X-Ray Fluorescence, using a Philips PW 2404 X-ray spectrometer with a rhodium anode (4 kW), in the laboratory of "S.A. Talc de Luzenac". The chemical composition of Pyro coll. was determined with a Cameca SX50 electron microprobe (Université Paul Sabatier, Toulouse). Operating conditions were 15 kV and 10 nA, natural and synthetic standards were used. X-ray diffraction data were obtained on a Philips X'Pert, using a reflection mode on powder preparations with Ni-filtered Cu K_α radiation (40 kV, 55 mA), in the laboratory of "Luzenac Europe". The same parameters were used for PP analysis on pressed films after melting, to obtain 50-μm thick films. B.E.T. specific surface areas (BETSSA) were determined on powders with a Micromeritics FlowSorb II 2300 under an Ar flow in the laboratory of "Luzenac Europe". The particle size d_{50} was determined using a Micromeritics SediGraph 5000ET in the laboratory of "Luzenac Europe". The average particle size d_{50} represents the median of the Gaussian distribution form of particles. Particles morphologies were observed on sample powders by SEM (Scanning Electronic Microscopy), using a LEO 435 VP, in the Ecole Nationale Supérieure de Chimie de Toulouse. Differential Scanning Calorimeter (DSC) analyses were performed on a NIETZCH 404. 500-μm thick PP pressed films were prepared and cut up to obtain discs of 5 mm diameter and a mass of about 15 mg. The samples were placed in an alumina crucible, heated up to 518 K and kept at this temperature for 10 min before cooling, using three cooling rates for each samples: 2.5, 5 and 10 K/min. This non-isothermal crystallizations ended near 350 K. PP crystallization observations were done using a ZEISS optical microscope under crossed polarizers and a wave accessory plate or with an Olympus Provis microscope equipped with a Sony video camera.

3. Results and discussion

3.1. Talc and pyrophyllite characterization

3.1.1. Chemical and mineralogical compositions

The chemical compositions of Italia and China talc samples are close to that of pure talc (Table I). Minor amounts of other oxides were detected for the other samples i.e., CaO for Spain talc, SiO_2 for Gabon talc and K_2O for pyro luz.

Traces of chlorite (<1%) in China and Italia talcs are detected by X-Ray diffraction (Fig. 1), whereas low amount of dolomite were found for Spain talc (<5%) and quartz in Gabon talc (<5%). Minor amounts of mica and kaolinite were also observed in pyro luz and pyro coll., respectively.

3.1.2. Physical and morphological characterization

All samples are characterized by various particle size d_{50} and BETSSA (Table II). Gradual particle size d_{50}

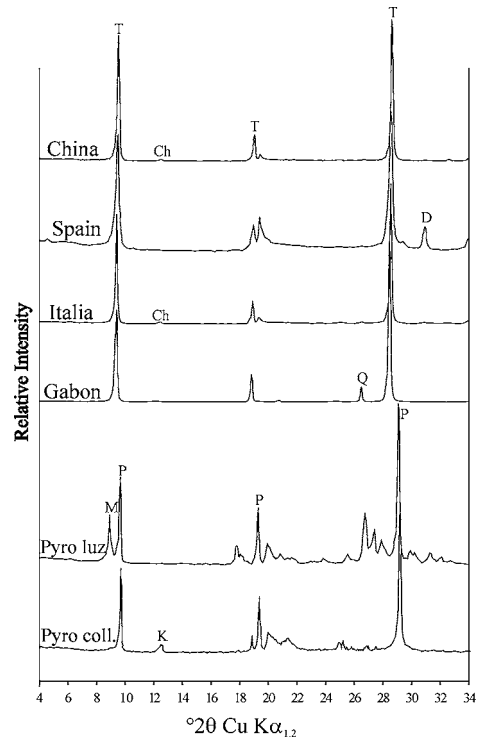

Figure 1 X-Ray diffraction data and mineralogical compositions of talc and pyrophyllite samples, with T: talc, Ch: chlorite, P: pyrophyllite, M: mica, D: dolomite, Q: quartz and K: kaolinite.

TABLE I Chemical analysis obtained by electron microprobe for Pyro. coll. and by X-Ray fluorescence for other sample powders

	Fluorescence weight oxide (%)					Electron microprobe (%)	
Product	China	Spain	Italia	Gabon	Pyro luz	Product	Pyro coll.
SiO_2	60.96	57.58	59.56	67.19	51.9	SiO_2	62.55
Al_2O_3	0.46	0.44	0.82	0.98	34.17	Al_2O_3	30.57
Fe_2O_3	0.09	0.37	0.74	0.15	0.11	FeO	0.44
MgO	31.58	29.82	30.48	24.61	0.09	MgO	0.08
CaO	0.21	1.82	0.58	0.04	0.19	CaO	0.02
K_2O	<0.01	0.01	0.015	<0.01	3.34	K_2O	0.04
Na_2O	<0.01	0.04	0.012	0.129	1.52	Na_2O	0.10
TiO_2	<0.1	<0.1	<0.1	<0.1	1.7	F	0.18
L.O.I.[a] (1050°C)	5.97	8.41	6.63	4.49	5.41	H_2O	4.52
Total	99.3	98.6	98.9	97.7	98.4	Total	98.5

[a]L.O.I. Loss on ignition.

TABLE II Particle size distributions and BET specific surface areas of talc and pyrophyllite samples

Product	China	Spain	Italia	Gabon	Pyro luz	Pyro coll.
Particle size distributions (μm)						
*d*95	4	2	7.7	23	13.5	20
*d*75	1.9	0.9	3.7	11.3	5	9.4
*d*50	1.1	0.54	2.2	5.6	2.15	4.2
*d*25	0.53	0.34	0.92	1.6	0.73	0.7
BET specific surface area (m^2/g)	16	60	21	7	17	45

is observed between 0.54 μm with a BETSSA close to 60 m^2/g for Spain talc and 5.6 μm with a BETSSA close to 7 m^2/g for Gabon talc. The decrease in size of particles involves an increase of the BETSSA, but for pyro coll., an anomalous strong BETSSA (45 m^2/g) is observed for a low particle size d_{50} (4.2 μm).

Morphological observations by SEM (Fig. 2a) show that Spain talc sample is constituted by very fine flakes, without arrangement, characteristic of microcrystallinity, while Italia and China talcs present macrocrystallinity with long, well stacked-up flakes (Fig. 2b and c). Gabon talc (Fig. 2d), formed by sepiolite

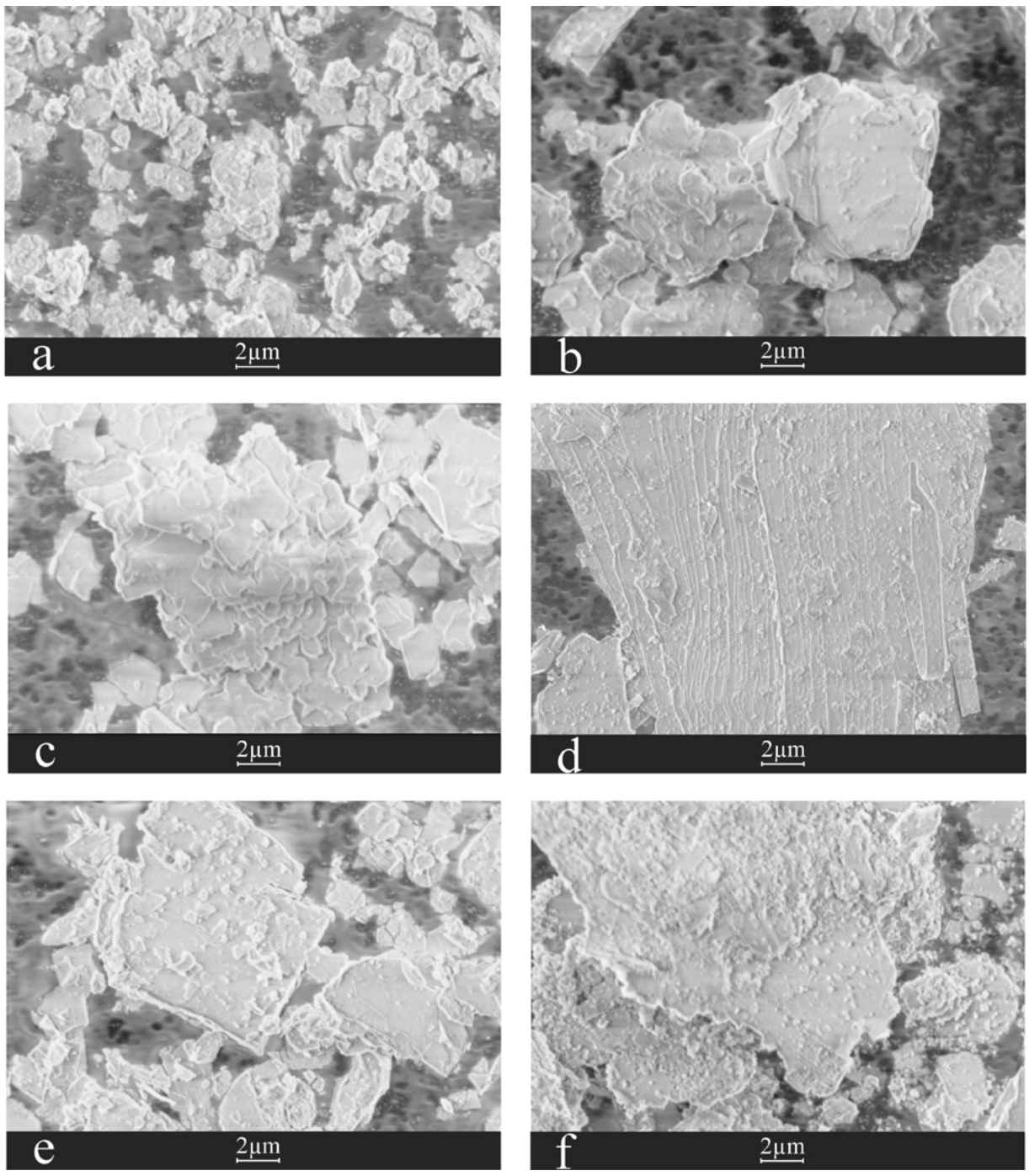

Figure 2 SEM images of the morphology of Spain (a), Italia (b), China (c), Gabon (d) talc samples and Pyro. luz (e), Pyro. coll. (f) pyrophyllite samples.

transformation, kept the sepiolite morphology with long and fine flakes arranged as "slates". The two pyrophyllites show macrocrystallinity but pyro coll. has more fines particles than pyro luz (Fig. 2e and f). This large number of fine particles is responsible of the strong BETSSA displayed by the pyro coll. sample.

3.2. Differential scanning calorimeter analysis of nucleated PP

DSC analysis of PP is a convenient technique for obtaining nucleation parameters informations with isothermal and non-isothermal kinetics [24].

In our study, we used the non-isothermal kinetics technic. DSC curves in Fig. 3 show the effect of adding 0.5% nucleating agent on PP for a cooling rate of 5 K/min. Addition of 0.5% nucleating agent (Spain talc or α nucleating agent) increased significantly the temperature of starting crystallization, called T° *onset*.

As the aim of this study is to characterize between all nucleating agents used, the differences of efficiency on the increase of T° *onset*, three cooling rates measurements on each compounds are reported in Fig. 4. These results permit to distinguish 4 individualized groups with various starting crystallyzation temperature (T° *onset*):

- stabilized (PPs) and unstabilized (iPP) PP as reference with weakest T° *onset*, indicating that stabilizing agent is not efficient on T° *onset*,
- Gabon talc and the two pyrophyllites which increase T° *onset* of PP (+∼5 K),
- Spain, Italia and China talcs are the most efficient talcs for increasing the temperature of starting crystallization of PP,
- the two organic nucleating agents α and β used as references in order to have the best efficiency on the increases of T° *onset*.

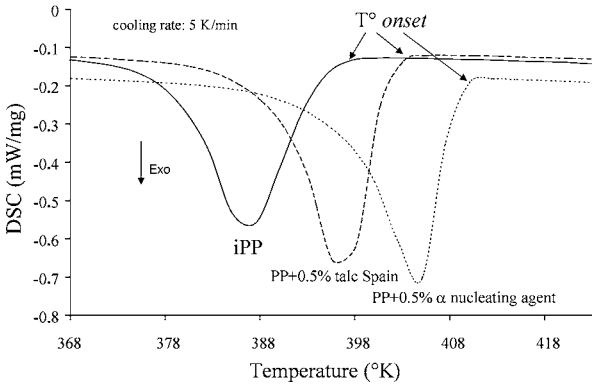

Figure 3 DSC crystallization curves for pure PP (——), PP with 0.5 wt% of talc Spain (— —) and α nucleating agent (. . . . . .).

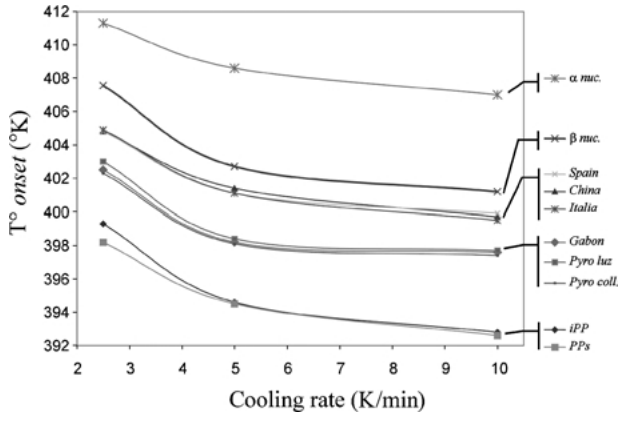

Figure 4 Influence of nucleating agents on PP T° *onset* for three different cooling rates (2.5, 5 and 10 K/min).

3.3. X-Ray diffraction patterns of nucleated PP

X-Ray scattering was used to characterize the effect of nucleating agents on PP orientation. For this study, composites samples are melted and pressed to realize 50-μm thick films. Under pressure, talc and pyrophyllite flakes are oriented parallel to the film surface, inducing an orientation of PP during crystallization. As for T° *onset* measurements, we seaked to determine which nucleating agent samples are efficient on the orientation of PP. Polypropylene α-form XRD patterns are characterized by 4 major reflections: (110), (040), (130), (111) at respectively 14, 17, 18.5 and 21.5°2θ with Cu $K_{\alpha 1,2}$. Only two reflections occur for the β-form: (300) and (301) located at °2θ with Cu $K_{\alpha 1,2} = 16$ and 21°, respectively [15]. XRD data on pressed films of unstabilized PP (iPP) reveals the four reflections of the α-form with intense (110) and (040) reflections (Fig. 5). The β-form can easily be observed on the PP β nuc. sample with the characteristic (300) reflection located at 16°2θ. Addition of 0.25% of stabilized agent in iPP (PPs) reveals a minor apparition of β-form. In this case, the stabilizing agent Irganox B225 induces crystallization of PP into the β-form. When a nucleating agent is added to the stabilized PP, some modifications in the crystallization of PP are observed: a decrease of the β-form induced by the stabilizing agent, and a variation in (110) and

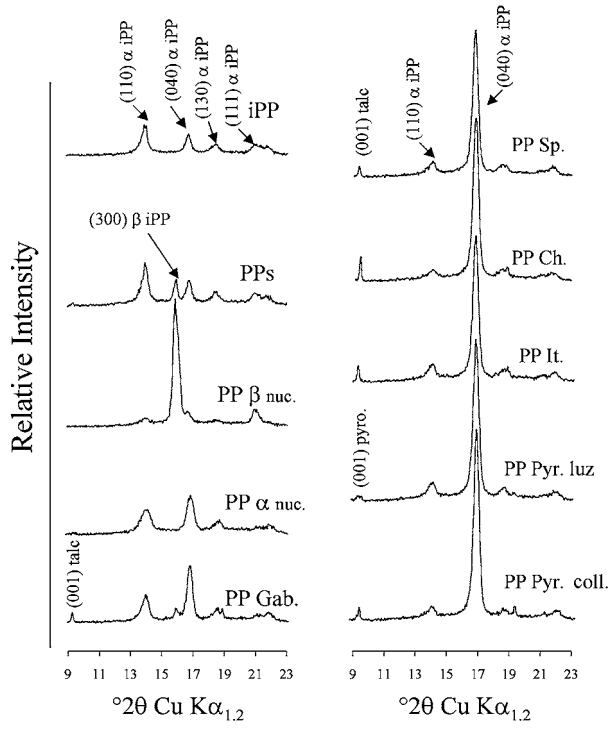

Figure 5 X-Ray diffraction data on non-nucleated and nucleated PP pressed films.

(040) intensities of α-form reflections. On PP α nuc. data, the β(300) reflection is clearly less intense than for PPs. Moreover, α(040) reflection is more intense than the α(110), while the contrary was observed for iPP and PPs data. For lamellar nucleating agent, the same phenomenon is observed. On PP Gab data, (001) reflection of talc is relatively strong, indicating at this low concentration (0.5%), that talc particles are oriented parallel to the pressed film surface. Observations of PP reflections show that β(300) reflection is present but that it is less intense than on PPs data and that α(040) is more intense than α(110).

In starting crystallization temperature measurements, Gabon talc seemed to be the least efficient nucleating agent on PP compared to the other talc samples, i.e., China, Spain and Italia talcs. On XRD data, we can note that China, Spain and Italia talcs are characterized by a very intense α(040), a very small α(110) and by the absence of β(300) reflection. The tendency of α(040) to increase and of α(110) to decrease when a nucleating agent is added, can be used to characterize the structural morphology of a PP composite. Lamellar particles are aligned parallel to the film surface (c^*-axis perpendicular to the surface), and PP crystallizes with a b^*-axis perpendicular to the film surface. In this way, c^*-axis of talc and pyrophyllite cells are merged with the PP cell b^*-axis. We propose that the nucleating efficiency of lamellar agent can be expressed as the intensity ratio between (040) and (110) reflections of the α-form [3, 11, 12].

3.4. Correlations

In order to characterize the parameters assuring the increase of starting crystallization temperature and oriented crystallization of PP, efficiency of all nucleating agents were compared. On T° *onset*, the most predominant factor appears to be the particle size d_{50}. Fig. 6 represents starting crystallization temperatures average for 5 K/min and 10 K/min cooling rates *versus* particles size d_{50}. We note that: (1) talc samples with finest particles sizes are the more efficient specimens increasing T° *onset*, and show a relatively good correlation (0.94 for linear regression); and (2) whatever the d_{50} value, the two pyrophyllites appear to be less efficient than the talc specimens.

Fig. 7 depicts a correlation between (110)/(040) reflection intensity ratio determined by XRD and the average of T° *onset* for 5 K/min and 10 K/min cooling rates. These results show that it is possible to have a linear relation between T° *onset* and the (110)/(040) ratio of talc samples, indicating that nucleation of PP is really effective on talc particles and that those two parameters can be used to characterize the efficiency of talc specimen on PP nucleation. The α organic nucleating agent plot is far off the correlation, due to the fact that his molecular particles are not oriented during the pressed film realization and that, in this case, PP orientation cannot be exacerbated by XRD. Finally, pyrophyllite samples appear to have a good effect on PP orientation, but are clearly less efficient on T° *onset* than talc specimens. The above results clearly show that particle size d_{50} is the principal parameter effecting T° *onset* when talc is used as nucleating agent in PP.

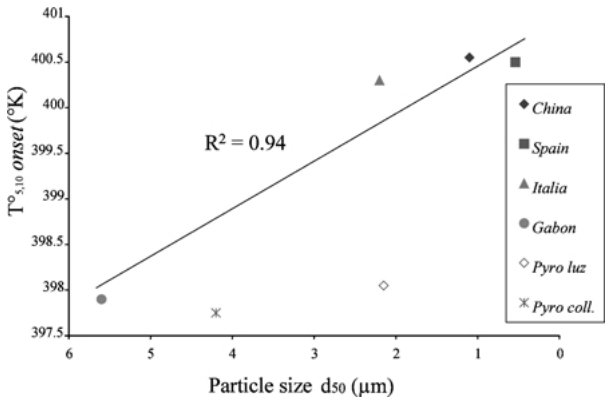

Figure 6 Influence of particle size d_{50} on T° *onset*.

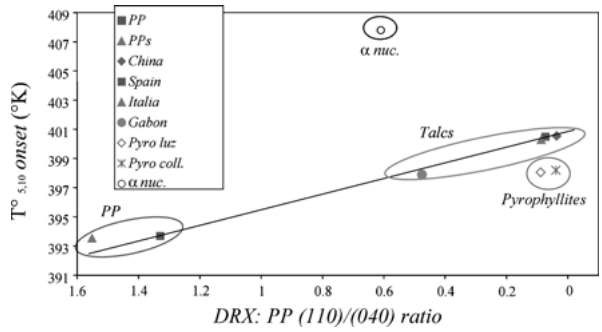

Figure 7 Correlation between T° onset average for cooling rates of 5 and 10 K/min and XRD (110)/(040) intensities ratio.

A comparison of the behavior of talc and pyrophyllite samples shows that PP oriented crystallization can be attributed to the lamellar form of these two minerals. XRD analyses revealed an epitaxial relationship between either talc and pyrophyllite, and PP during its crystallization. Nevertheless, although talc and pyrophyllite have the same effect on PP oriented crystallization, there are differences in the starting temperature of crystallization. Whatever the particle size d_{50} and with the same lamellar form of particles, PP samples containing talc always have a higher crystallization temperature than PP containing pyrophyllite. This information reveals a better structural affinity of PP with talc than with pyrophyllite in first steps of PP crystallization. The onset of crystallization, which can be attributed to the alignment of few PP chains before the epitaxial growth, depends in this case on the crystallographic nature of substrate, and notably the structural mineral surface, which is more corrugated on pyrophyllite than on talc.

3.5. Optical microscope observations of PP crystallization

In the preceding sections we have seen that addition of a nucleating agent modifies the crystallization process of PP. This consists of an increase in the starting crystallization temperature and the appearance of a structural orientation in PP. In order to characterize the morphological modifications in PP induced by the presence of talc, the PP crystallization process was observed in detail by optical microscopy. For this purpose, a 25-μm thick pressed polymer film was melted at 523 K for 10 min and an isothermal crystallization was realized

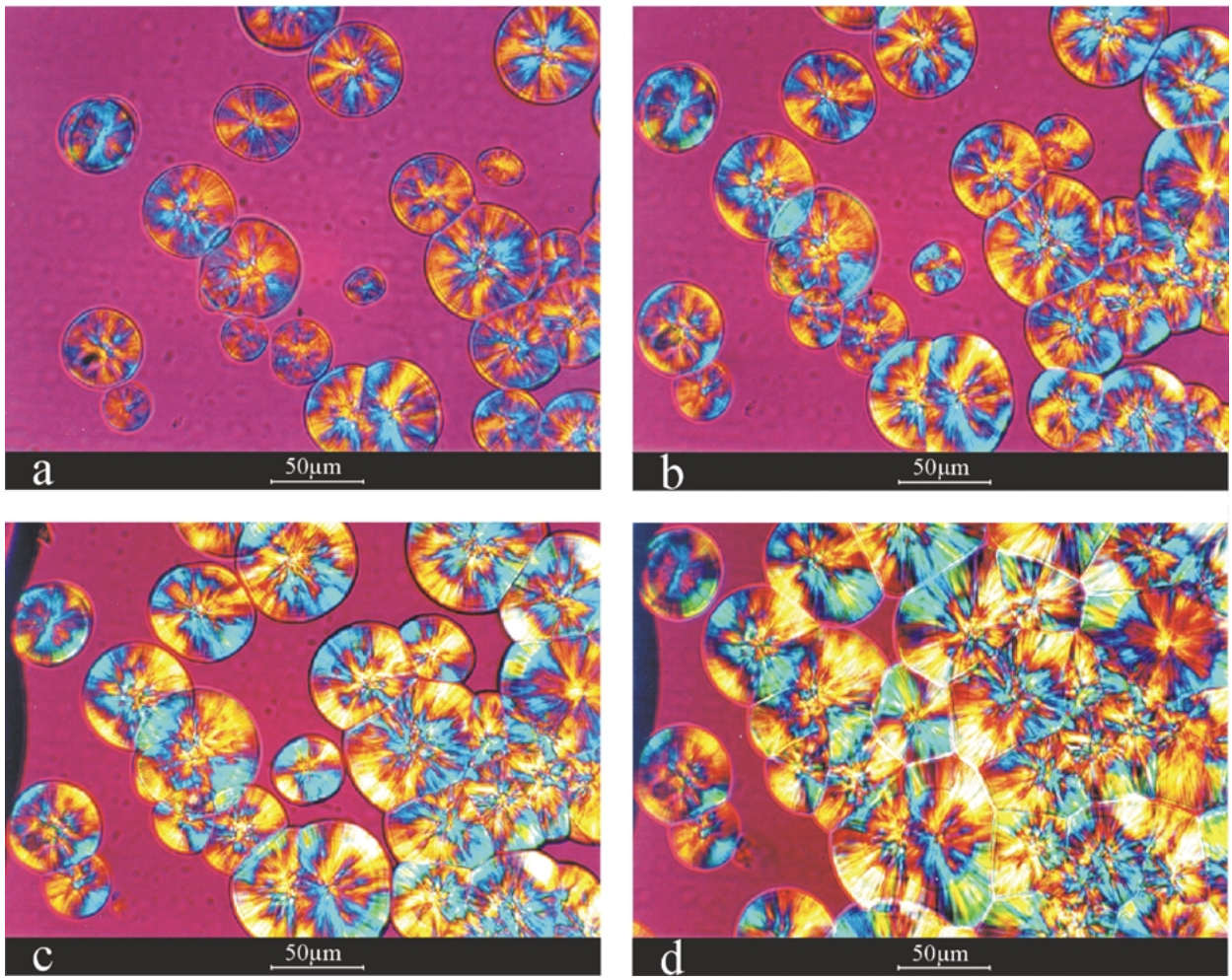

Figure 8 Optical microscopic observations of the non-nucleated PP isothermal crystallization, after 15 min (a), 35 min (b), 1 h 05 min (c) and 1 h 55 min (d).

at 473 K. Fig. 8a–d (obtained with a ZEISS microscope) show different time snaps of iPP crystallization without nucleating agent. After 15 minutes of crystallization, few spherulites appear, and are well distributed in the polymer matrix melt (Fig. 8a). The growth of those spherulites is slow, and after 2 hours the sample is not yet completely crystallized (Fig. 8d).

When 0.5% of Italia talc is added (PP Italia), talc particles become visible in the polymer melt (Fig. 9a–d). Compared to the previous sample, after a 15 min interval, a large number of spherulites were observed, induced by the nucleating agent (Fig. 9b). Therefore, presence of talc particles cause an increase of nuclei density. In this case, crystallization is completed after only 50 min and the sample is characterized by very small spherulites compared to pure PP (Fig. 9d). These observations show the importance of fine talc particles, which, well distributed into the polymer melt, can induce a large concentration of PP nucleation germs. In this scenario, crystallites are well distributed producing a final material characterized by a well homogeneous texture. Nevertheless, it is difficult to determine whether the first PP germs nucleate, on particle surfaces or on particle steps. The heterogeneous nucleation mechanism was first described in the literature as a "nucleation at steps of limited length of the nucleation particles where ditches in the latter can cause prealignment of polymer chains" [25]. In order to observe the location of the first crystallites, optical microscopic observations of PP crystallization were realized (with an Olympus Provis microscope) on a large talc flake, using the same parameters as in previous experiences. We used talc from Brazil, which is characterized by long, well stacked-up flakes (Fig. 10). For this experience, a 25-μm thick pressed film of pure PP was realized, placed on the talc lamellae and then melted at 523 K for 10 min. Isothermal crystallization was studied at 473 K, under the same conditions. Observations, above plain polarized light, reveal a talc lamellae in the polymer melt (Fig. 11a). In Fig. 11b, the polarizers are crossed and the isotropic PP melt appears in black. After 20 min, many crystallites appear as white spots, and concentrate on talc lamellae surface (Fig. 11c). In Fig. 11d, we can observe the difference in nuclei density distribution between talc surface and polymer matrix: the talc surface is entirely covered by polymer and no specific crystallization directions are observed. After 1 h (Fig. 11e), the crystallization on talc surface seems to have ended, while after 2 h, the matrix is still not completely crystallized (Fig. 11f). This last figure also shows a difference in PP crystallites size, which form small spherulites on talc surfaces but large ones in the matrix.

These results do not permit PP nuclei to be clearly located on steps or defects of particles. Using a large talc lamella, crystallites seem to appear everywhere on

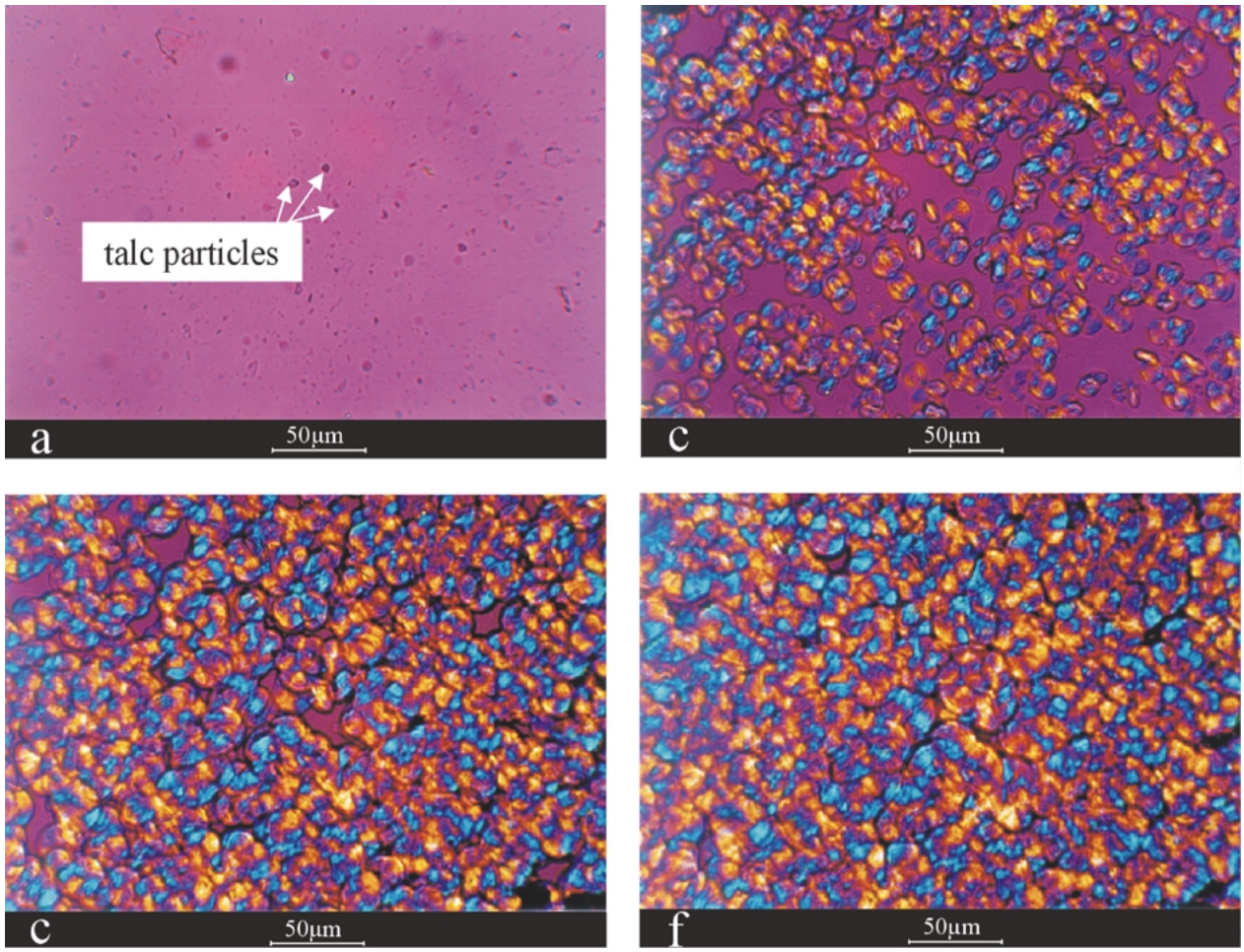

Figure 9 Optical microscope images of isothermal crystallization for the nucleated PP with 0.5% Italia talc at $t = 0$ min (a), after 15 min crystallization (b), 30 min (c) and 50 min (d).

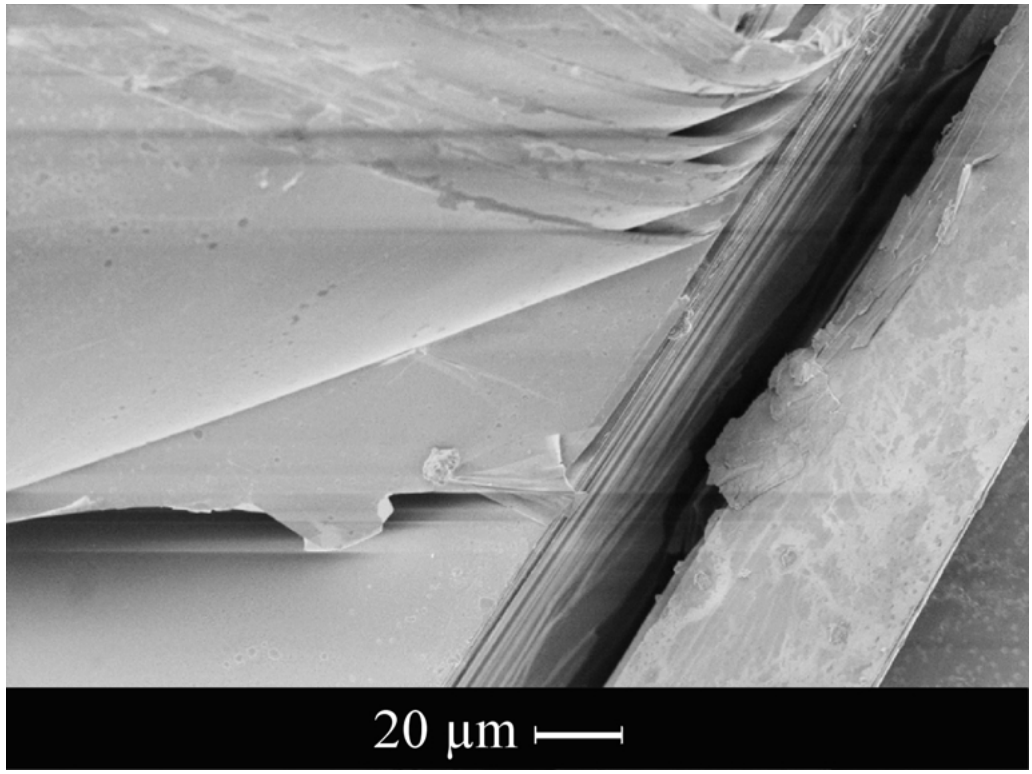

Figure 10 SEM observation of talc from Brazil constituted by very long, perfectly stacked-up flakes.

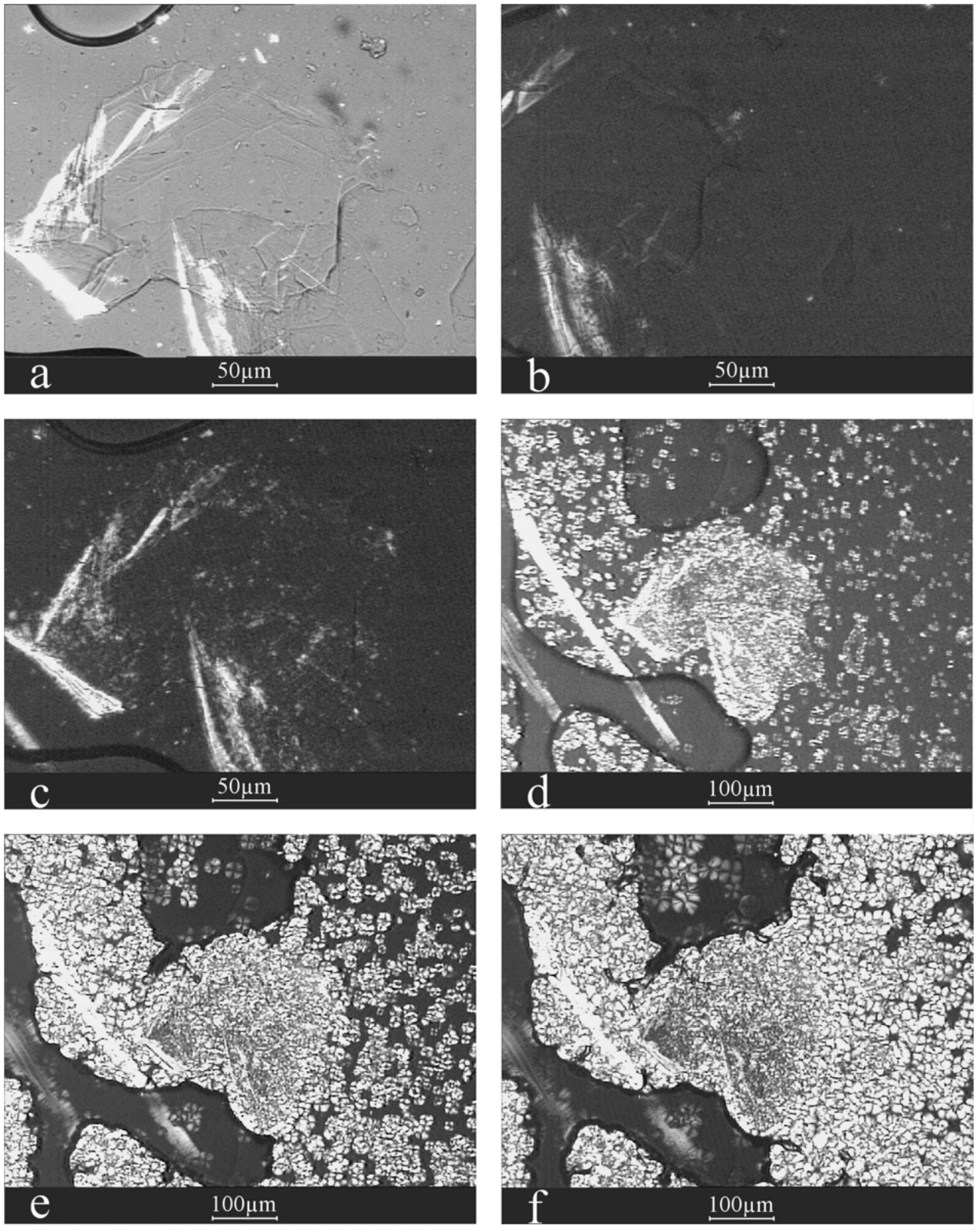

Figure 11 Optical microscope images of PP isothermal crystallization on a large flake of talc from Brazil under plain polarized light at $t = 0$ min (a) and under crossed polarizers at $t = 0$ min (b) and after 20 min (c), 40 min (d), 1 h 15 min (e), 1 h 45 min (f).

particle surface and principally on the basal surface of talc sheets. Previous results, showing a better talc-PP than pyrophyllite-PP affinity for the first moments of crystallization, involve the importance of the mineral structural surface, the crystallographic parameters, surface corrugation (in pyrophyllite) and chemical affinity of mineral with PP. In this case, it is necessary to consider the epitaxial relation between the mineral and the PP crystallites as a fine structural relation between PP chains alignment and surface of tetrahedral sheet of talc and pyrophyllite.

3.6. PP-talc interface modelization

Previous studies on the importance of the substrate during heterogeneous polymer nucleation took into

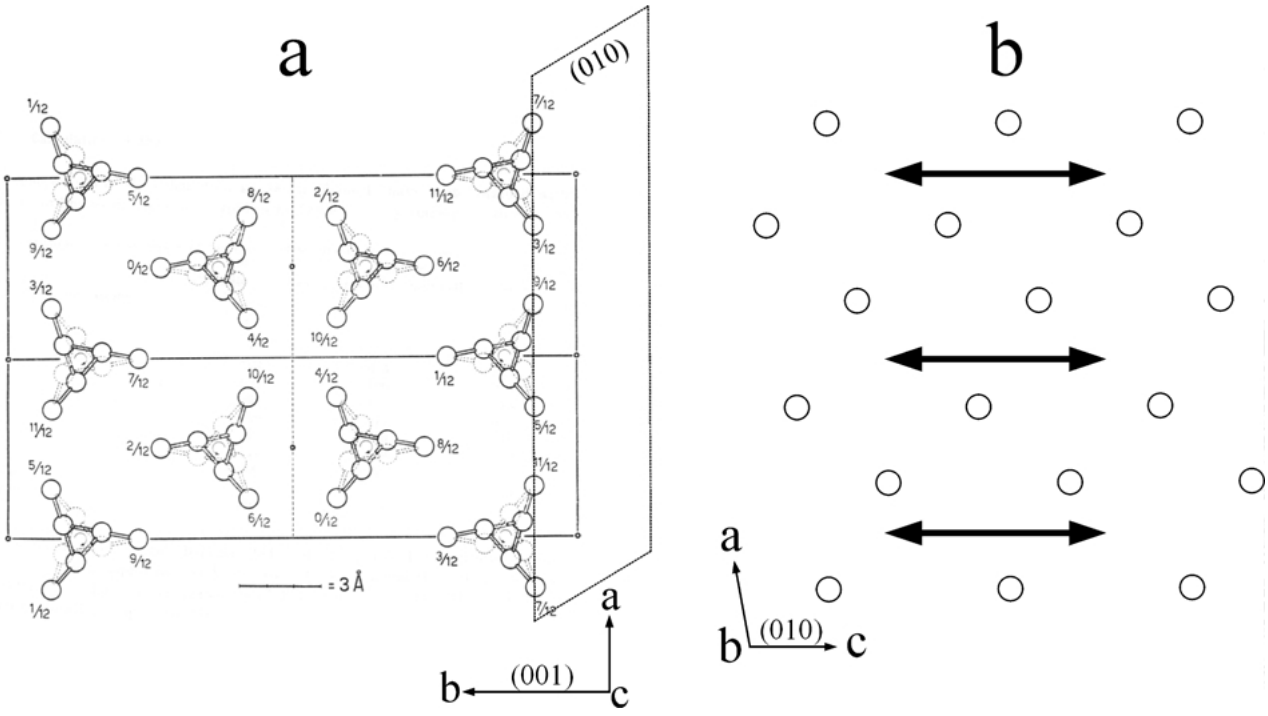

Figure 12 Isotactic α-form of the PP structure. In this representation only the carbon helix is represented (a). Projection of the αPP structure the (a, c) plane and representation of the PP chains elongation (b).

account the importance of the similarity of crystallographic unit cell between polymer and substrate for the epitaxial phenomenon [26]. X-Ray results, reported here show that when talc is added to PP, crystallization on talc particles has an epitaxial relationship characterized by a strong orientation of PP (increase of the (040) reflection) to accommodate talc and PP cells. Microscope observations reveal clearly that numerous PP nuclei appear everywhere on the talc surface. These results are in accordance with the previously proposed mechanism [26] whereby the crystallographic similarities are considered as the principal condition for epitaxial relation. In our study, the similarity of the talc cell (in the (a, b) plane) to the PP cell (in the (a, c) plane) could induce PP crystallization at the talc surface with a preferred orientation (b^* axis of PP merged with c^* axis of talc). This description can also be applied for the pyrophyllite-PP relation, but in pyrophyllite the (a, b) plane on tetrahedral surface sheets is corrugated. We will now focus on the PP-talc interface, notably on the modelization of the epitaxial phenomenon. The αPP structure is represented by the carbon helix in the *C/c* space group, as described by Natta and Corradini [27] (Fig. 12a). The talc structure was reconstructed using CaRIne Crystallography 3.1 software, with the atomic positions described by Perdikatsis [20]. The first representation of the talc structure along the c^* axis (Fig. 13a) shows the octahedral sheet sandwiched between the two tetrahedral sheets. The second representation shows the structural surface of tetrahedral sheet on the (a, b) plane (Fig. 13b), with the tetrahedral rotation angle α around 3.6°. In this ditrigonal representation, hydrogen atoms are linked to oxygens of the octahedral sheet, inside the hexagonal cavity. On the talc surface, oxygen atoms which link the tetrahedra have four electronic orbitals: two oriented towards the silicon atoms inside the two adjacent tetrahedra, and the other two toward the center of two hexagonal rings at the exterior of the talc surface (Fig. 14). The hexagonal rings in this case can be considered as electronegative sites, propitious to realize a hydrogen bond with the methyl grouping of PP. According to the XRD results, when talc or pyrophyllite is added to the polymer, PP crystallizes with a b^*-axis merged with the c^*-axis of the mineral (Fig. 5). At the talc-PP interface we can consider the matching of two atomic planes:

– for talc, the basal oxygen plane at the surface of tetrahedral sheet,
– for PP, the (010) atomic plane composed by carbon atoms, representing 2 carbons from 3 which participate of CH_3 groupings (Fig. 12b).

If those two planes are joined, it is possible to observe a fine structural relation between talc and PP (Fig. 15). In our model, one every two methyl groups from the (010) PP plane can be bonded by an oxygen atom linking two tetrahedra, the other can be situated on the hexagonal ring of talc, the more attractive site on the talc surface, to form an hydrogen bond. This structural relation is possible with only 3% accommodation of PP cell on talc surface. An angle of around 15° between the a or b talc axis and an elongation chain of PP (c^*-axis) permit the fitting and can explain the good relationship between talc and PP. It is possible to understand the great efficiency of talc on PP as nucleating agent or filler, with this model, and the difference between talc and pyrophyllite. When talc is present in PP, we suggest that during crystallization only a few PP chains can align themselves on talc surface as proposed in the model, thus causing the apparition of a nucleus site on the mineral surface. The substrate can influence

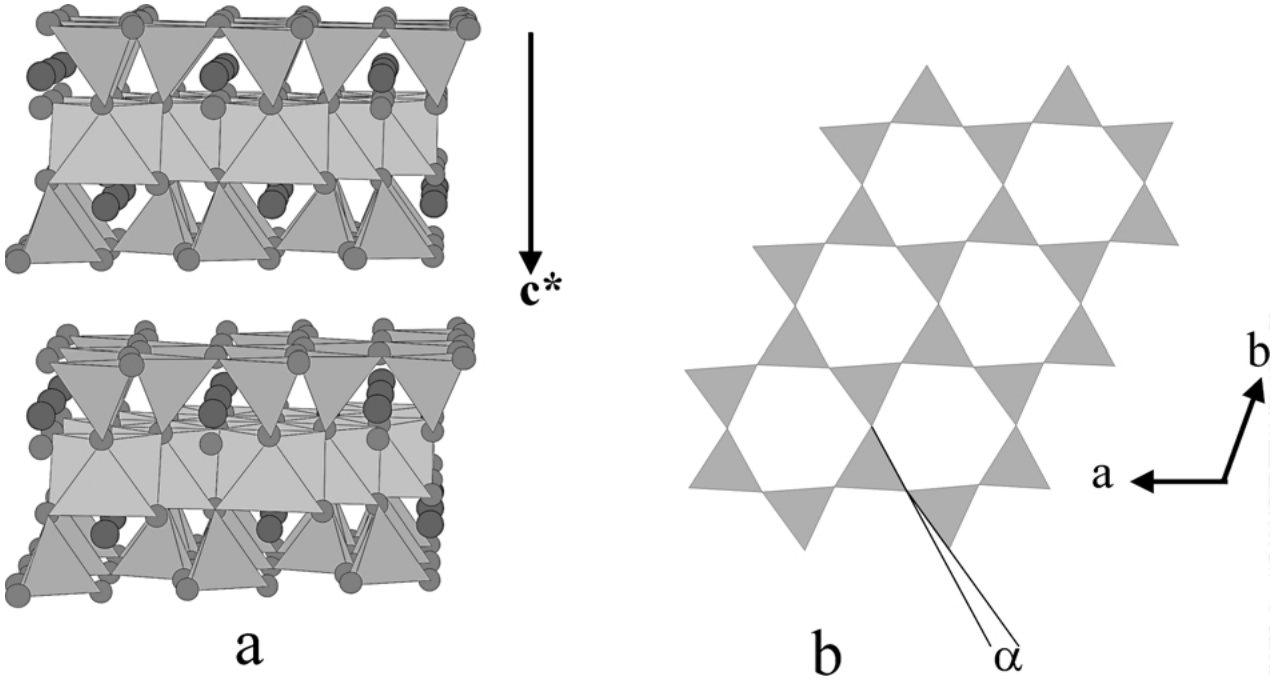

Figure 13 Talc structure reconstructed with the CaRIne Crystallography 3.1 software along the c^*-axis (a) and in the (a, b) plane (b).

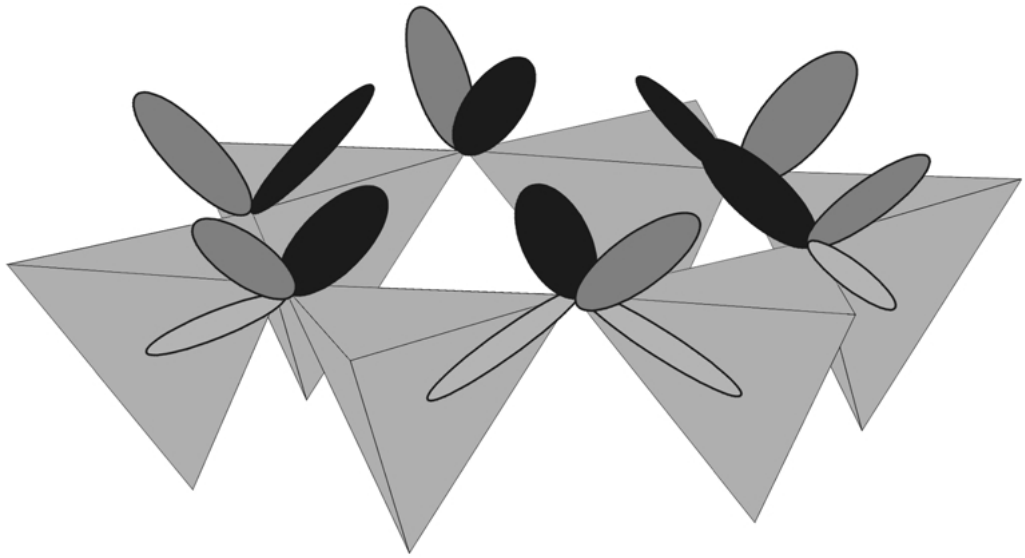

Figure 14 Representation of oxygen molecular orbitals above the hexagonal ring on talc basal surface.

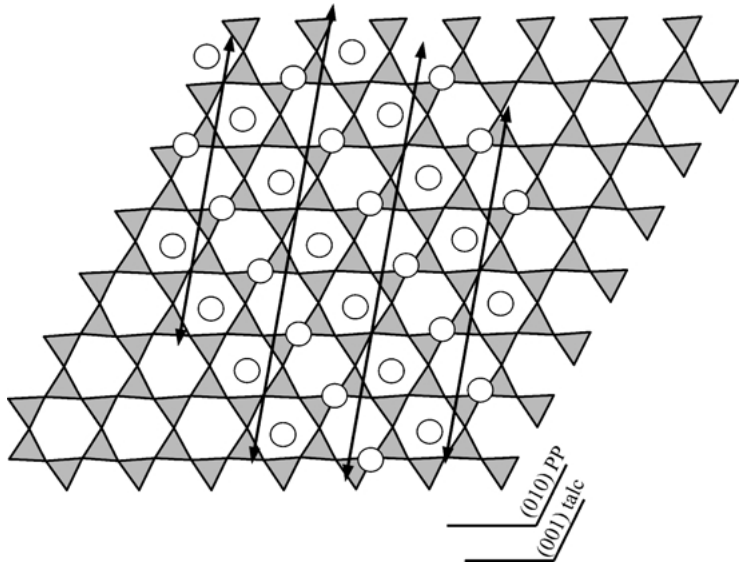

Figure 15 Modelization of the PP-talc interface, superposing (001) talc plane and the (010) PP plane.

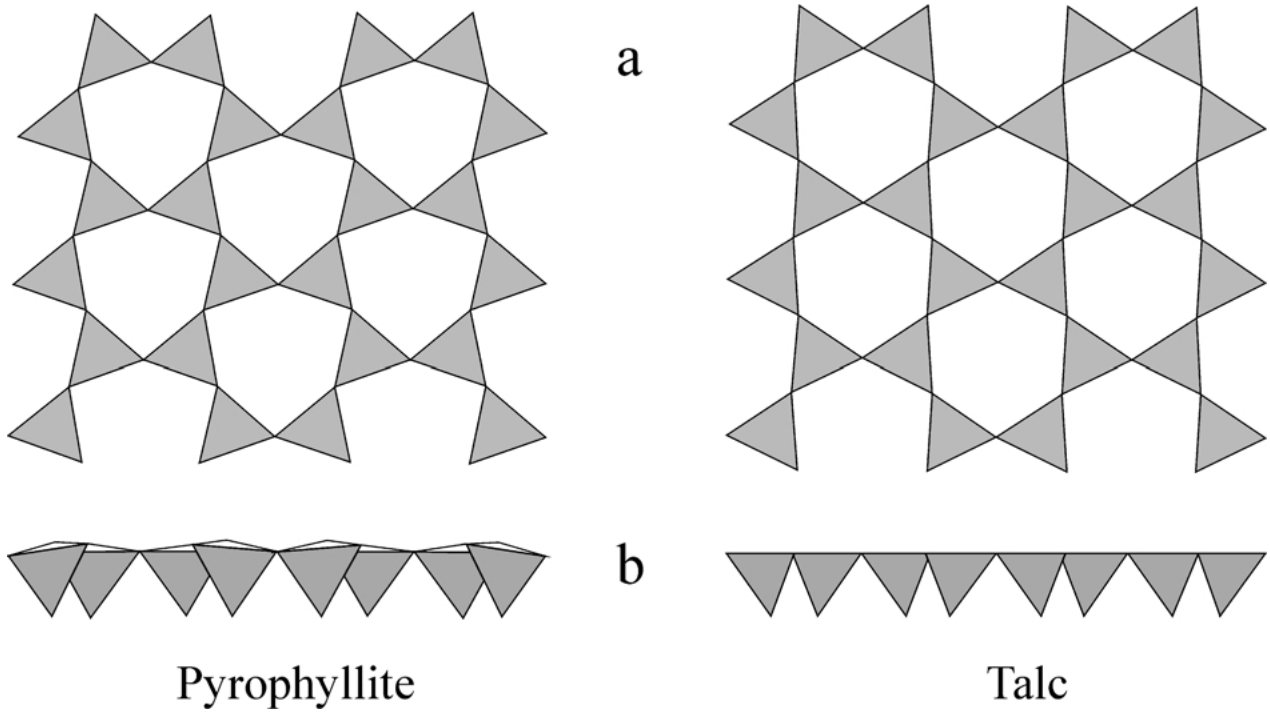

Figure 16 Comparison of the talc and pyrophyllite structures in the (a, b) plane (a) and along the c^*-axis (b).

crystallites growth into a particular orientation (PP b^*-axis merged with talc c^*-axis) which, together with a nuclear density increase, will shorten the duration of the crystallization process.

We show that pyrophyllite also causes PP to be oriented, but that there is a difference in crystallization temperature onset, attributed to a better talc-PP than pyrophyllite-PP affinity during the beginning of crystallization. This difference can be explained by the structural surface differences between the two minerals. Differently from talc, the presence of a strong tetrahedra rotation on the (a, b) plane (Fig. 16a) and of a corrugation on the pyrophyllite surface (Fig. 16b) can interfere with the alignment of the first PP chains on the pyrophyllite surface, inducing a lower starting crystallization temperature. Accommodation of PP on the pyrophyllite surface is possible, but with a greater distortion than in the case of talc. Once the joining is realized, the crystallization phenomenon can take place, as is the case for talc, with a great orientation.

4. Conclusions

In polymer industrial applications, talc in polypropylene has proved to be particularly efficient on thermal and mechanical properties of the resulting compound. On one hand, talc addition to a polymer causes a rising of PP crystallization temperature, on the other hand, it induces an oriented crystallization of PP. The efficiency of different talc samples with varied physical characteristics (particles size distribution and BET specific surface area) were compared to pyrophyllite samples. These present a structure similar to that of talc but with distortions on their surfaces. Talc samples were also compared to two organic nucleating agents (α and β nucleating agents). Our study showed that the principal parameter controlling the efficiency of talc addition in increasing the starting crystallization temperature is its particles size distribution. Independently of particle size d_{50} or BET specific surface area, in addition, talc revealed more efficient than pyrophyllite, showing a better affinity with PP than pyrophyllite at the onset of crystallization. The orientation phenomena due to these additions of these minerals were studied on PP nucleated pressed films by X-ray analyses. Addition of talc or pyrophyllite induces an increase of the (040) reflection and the decrease of the (110) reflection. In this orientation, the c^*-axis of talc or pyrophyllite is merged with the PP b^*-axis, which is a characteristic phenomenon of an epitaxial growth of PP crystallites on the mineral crystallographic surface. Microscope observations clearly showed an increase of nuclei density when talc is added to PP as a nucleating agent. PP crystallization observations on a large talc flake revealed that nuclei appear everywhere on the talc surface, involving the role of substrate and more particularly of the crystallographic structure on talc surface. A PP-talc interface structure modelization is proposed involving the matching of (001) talc plane and the (010) PP plane. The proposed model envisages a 15° angle between PP chains elongation and the mineral crystallographic directions, with only 3% of accommodation of the PP cell on the talc one. In this representation, we suggest the presence of hexagonal rings on tetrahedral talc sheet, in order to form hydrogen bonds with the PP methyl groupings. With this representation, differences of efficiency observed between talc and pyrophyllite can be explained. More distortions on pyrophyllite surface could interfere the alignment of chains on the mineral surface, inducing a lower efficiency of pyrophyllite on the increase of starting crystallization temperature than for talc, but when the matching of first chains is realized, the epitaxial crystallization can induce as for talc, a particular orientation. In our study we focused

on physical parameters controlling the efficiency of talc and differences observed with pyrophyllite. All results bring us to take into account the talc surface structure to propose an interface model. This modelization could permit to better understand the efficiency of talc on PP properties and anticipate the lower efficiency of others lamellar minerals as pyrophyllite, micas.

References

1. SHUCAI LI, P. K. JÄRVELÄ and P. A. JÄRVELÄ, *J. Appl. Polym. Sci.* **71** (1999) 1641.
2. *Idem.*, *ibid.* **71** (1999) 1649.
3. F. RYBNIKÁŘ, *Eur. Polym. J.* **27** (1991) 549.
4. B. PUKÁNSKY, K. BELINA, A. ROCKENBAUER and F. H. J. MAURER, *Composites* **25** (1994) 205.
5. B. FILLON, A. THIERRY, B. LOTZ and J. C. WITTMAN, *J. Therm. Analys.* **42** (1994) 721.
6. J. MENCZEL and J. VARGA, *ibid.* **28** (1983) 161.
7. A. M. CHATTERJEE and F. P. PRICE, *J. Polym. Sci: Polym. Phys. Ed.* **13** (1975) 2385.
8. J. I. VELASCO, J. A. DE SAJA and A. B. MARTÍNEZ, *Revista de Plasticos Modernos num.* **477** (1996) 271.
9. F. L. BINSBERGEN, *J. Polym. Sci: Polym. Symp.* **59** (1977) 11.
10. B. E. TIGANIS, R. A. SHANKS and YU LONG, in *ANTEC '96* (1996) p. 1744.
11. M. ALONSO, A. GONZALEZ and J. A. DE SAJA, *Plast., Rub. Comp. Proc. and Appl.* **24** (1995) 131.
12. M. FUJIYAMA, *Intern. Polym. Processing* **XIII** (1998) 406.
13. E. MORALES and J. R. WHITE, *J. Mater. Sci.* **23** (1988) 3612.
14. F. RYBNIKÁŘ, *J. Appl. Polym. Sci.* **38** (1989) 1479.
15. A. TURNER JONES, J. M. AIZLEWOOD and D. R. BECKETT, *Imp. Chem. Indust. Lim.* (1963) 134.
16. J. VARGA and J. MENCZEL, *J. Therm. Anal.* **35** (1989) 1891.
17. M. FUJIYAMA, *Intern. Polym. Processing* **XIII** (1998) 284.
18. J. W. GRUNER, *Zeit. Krist. Kristallgeom.* **88** (1934) 412.
19. J. H. RAYNER and G. BROWN, *Clays Clay Miner.* **21** (1973) 103.
20. B. PERDIKATSIS and H. BURZLAFF, *Z. Kristallogr.* **156** (1981) 177.
21. E. W. RADOSLOVITCH, *Amer. Miner.* **47** (1962) 599.
22. B. W. EVANS and S. GUGGENHEIM, *Reviews in Miner*; Vol. 19, edited by S. W. Bailey (1988) p. 226.
23. J. HOO LEE and S. GUGGENHEIM, *Amer. Miner.* **66** (1981) 350.
24. K. KISHORE and R. VASANTHAKUMARI, *Colloid Polym. Sci.* **266** (1988) 999.
25. F. L. BINSBERGEN, *J. Polym. Sci: Polym. Phys. Ed.* **22** (1973) 117.
26. A. M. CHATTERJEE, F. P. PRICE and S. NEWMAN, *ibid.* **13** (1975) 2369.
27. G. NATTA and P. CORRADINI, *Nuov. Cimento.* **1** (1960) 40.

Received 13 April
and accepted 4 December 2001